Mem. S.A.It. Vol. , 1

Memorie della

Preliminary test results of the UTOV Fabry-Pérot interferometer prototype

L. Giovannelli, F. Berrilli, M. Cocciolo, D. Del Moro, A. Egidi, R. Piazzesi, and M. Stangalini

Dipartimento di Fisica, Università di Roma "Tor Vergata", Via della Ricerca Scientifica, I-00133 Rome, Italy, e-mail: `giovannelli@roma2.infn.it`

Abstract. We present the numerical model and the general mechanical description of a narrow-band optical filter prototype developed at the Tor Vergata University (UTOV). The prototype is a Capacitance Stabilized Etalon (CSE), i.e. a spectrometer with imaging capabilities and the possibility to scan the source spectrum with a resolving power of about 58000 and a center-band minimum step of $7pm$. These characteristics, combined with the high transparency (59.8%) of the instrument, make it suitable to study the fast dynamic of solar atmosphere. The design provides a coarse and fine instrument control, based on motorized micrometers and piezo-actuators, allowing for fast (1ms) tuning capabilities. We present general mechanical behaviour for the protoype that has been tested for an optical bench use and possible applications at the focal plane of a ground based telescope. These studies have been performed and in the perspective of a new space-qualified prototype for satellite use. The developed prototype is part of the study for the narrow band channel of the ADvanced Astronomy for HELIophysics (ADAHELI) mission. ADAHELI is a solar satellite designed to investigate the dynamics of solar atmosphere as part of the Italian Space Agency (ASI) program. A proposal based on ADAHELI was submitted to ESA S-class Mission 2012 Call.

Key words. Instrumentation: interferometers – Techniques: spectroscopic – Space vehicles: instruments – The Sun

1. Introduction

Fabry-Pérot tunable filters allow the scanning of spectral lines in an extended range of wavelengths. They are an excellent tool for high spectral resolution imaging for both ground-based and space applications (Kameda et al. 2010).

The prototype here presented has been developed as part of the study for the narrow band channel of the ADAHELI mission. A laboratory prototype has been tested for general mechanical behavior, in order to understand the feasibility of a space Fabry-Pérot interferometer.

2. The ADAHELI mission

ADAHELI is a small-class low-budget satellite mission; the main aim is to monitor solar flares and to study the dynamics of different layers of the solar atmosphere (Berrilli et al. 2009, 2010). ADAHELI design has completed its

Send offprint requests to: L. Giovannelli

Phase-A feasibility study in December 2008, in the framework of ASI (Agenzia Spaziale Italiana) 2007 Small Missions Program. The University of Rome “Tor Vergata” is the leading scientific institution of the project and CGS SpA is the leading industrial partner.

The ISODY (Interferometer for SOlar Dynamics) instrument is the main payload of the satellite (Greco et al. 2010). It is designed to obtain polarimetric images of the solar photosphere and chromosphere with high spatial, spectral, and temporal resolution. The Focal Plane Assembly (Berrilli et al. 2011) of the ISODY instrument comprises two visible near-infrared science optical paths or channels: the Narrow Band (NB) and the Broad Band (BB) channels. The principal optical path of the NB channel includes two FP interferometers used in axial-mode and in classic mount.

3. Prototype parameters choice

3.1. The ideal Fabry-Pérot

The transmission profile depends on the value of the reflectivity R, the reflecting finesse $\mathcal{F}_R$ and the interference order m (Born & Wolf 1999) :

$$\mathcal{F}_R = \frac{\pi\sqrt{R}}{1-R} \tag{1}$$

$$m = \frac{2n}{\lambda} d \cos\theta \tag{2}$$

The order m, once defined the working wavelength, depends on the refracting index n, the angle of incidence θ and the gap spacing d. The reflecting finesse depends only on the reflectivity R and is set choosing a suitable multilayer dielectric coating. The Free Spectral Range (FSR, is the distance between consecutive orders peaks) and FWHM of the transmission peak are then:

$$FSR = \frac{\lambda}{m} \tag{3}$$

$$FWHM = \frac{FSR}{\mathcal{F}_R} \tag{4}$$

These are the parameters that define the characteristics of a FP-based spectrometer.

3.2. The effective Fabry-Pérot

Key issues for a plane parallel interferometer are the defects of the plates, a not perfect parallelism and the effects of a not perfectly collimated beam. They cause a broadening of the spectral profile which can be taken into account in term of finesse.

We can model the effect of a not perfectly flat plate using the spherical defect finesse $\mathcal{F}_{DS}$. Aside from systematic surface defects, a surface rugosity is always present after the plate has been polished. Under the hypothesis of Gaussian distributed residuals errors on the surface, they can be described with $\mathcal{F}_{DG}$ finesse. The parallelism defect finesse $\mathcal{F}_{DP}$ takes into account the effect generated by not perfectly parallel plates. If the incident beam has a certain amount of divergence, the difference of incidence angles between inner and outer rays will also broaden the transmission profile. This effect is called the aperture finesse $\mathcal{F}_{DIV}$.

All previous definitions of finesse can be included in the effective finesse $\mathcal{F}_E$ which describes an effective interferometer. A more detailed description can be found in Giovannelli et al. (2012).

$$\mathcal{F}_E = \left(\frac{1}{\mathcal{F}_R^2} + \frac{1}{\mathcal{F}_{DS}^2} + \frac{1}{\mathcal{F}_{DG}^2} + \frac{1}{\mathcal{F}_{DP}^2} + \frac{1}{\mathcal{F}_{DIV}^2} \right)^{-\frac{1}{2}} \tag{5}$$

3.3. Numerical simulation

We developed a software model to simulate the performance of the prototype and we used the $\mathcal{F}_E$ term to account for the effective behaviour of the system. We simulated three FPs, with three different gap widths d: 0.3 mm, 1.0 mm and 3.0 mm (Fig.1). The broadening of the transmission profiles and the drop in transparency for the effective cases is rather evident (Peak transparency = 59.8%). The simulation aim was to decide which d value made the instrument more suitable to scan the H_α line. In a trade-off between the FSR and Resolving Power (RP), using equation 4, we selected the $d = 1.0$ mm value, corresponding to $FSR = 0.215nm$, $FWHM = 11.2pm$ and $RP = 58589$ (see Giovannelli et al. 2012).

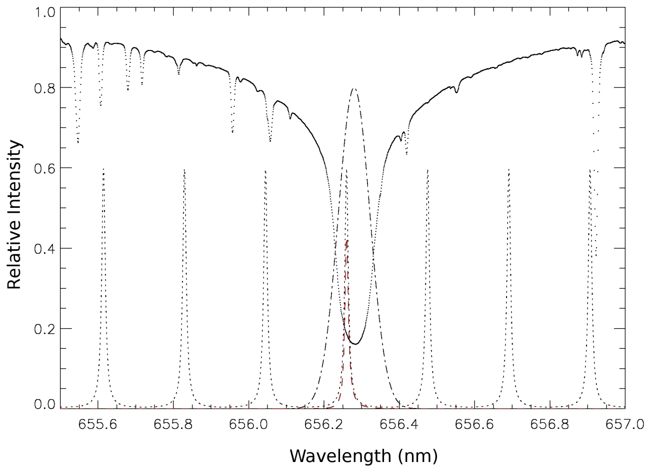

Fig. 1. FP numerical simulations with d=1 mm. Effective FP profile (dashed); H_α absorption line (dotted); prefilter profile (dot-dashed); FP + prefilter (red).

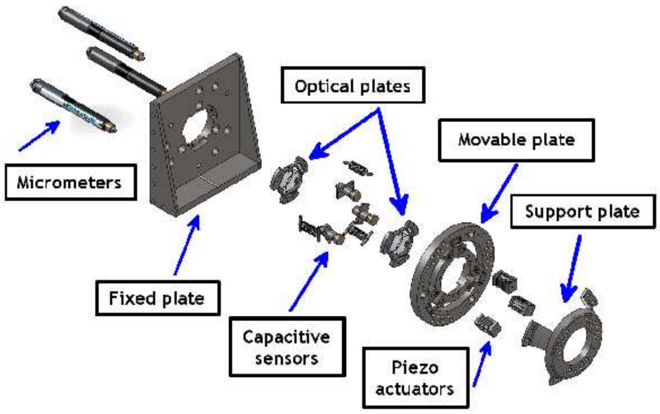

Fig. 2. Prototype exploded view.

4. Prototype design

To study the feasibility of a space-qualified FP, we realized a scanning optical cavity with a gap servo control system.

We have designed the optomechanics of the FP prototype to house: a pair of 1" (25.4 *mm*) partially reflecting mirrors, three micrometers, three piezoelectric actuators, three high sensitivity capacitive sensors, with a 120°-symmetry around the etalon (See Fig. 2).

The micrometers allow for a coarse adjustment of the gap width, up to $\pm 12mm$. The piezo-actuators allow for a finer adjustment, with a maximum extension range of $15\mu m$, while the capacitive sensors working distance is $50\mu m$.

The gap width can be varied either with the piezo-actuators or with the micrometers, since

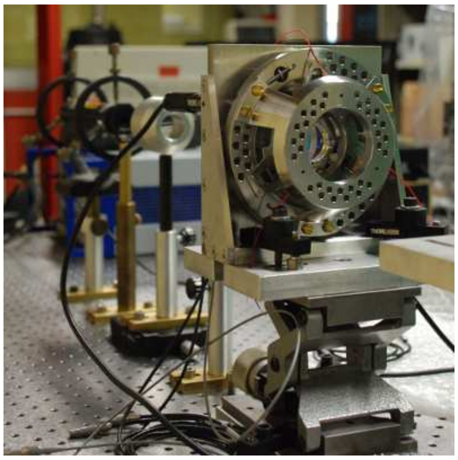

Fig. 3. Assembled prototype on the optical table for mechanical and optical tests.

the prototype has been designed to decouple these two different adjustment by separating the movable plate into two concentric rings.

The main requirements for this device are to allow a fast variation of the gap within the semi-reflecting plates, while maintaining their parallelism within the tolerances. In addition, positioning repeatability must be guaranteed in order to obtain the same spectral points in successive measures.

To achieve these goals, we employ piezoelectric actuators to change the gap spacing and capacitive sensors to monitor its width. The combination of these two technologies in a servo controlled system grants the necessary stability and repeatability ($\lambda/3000$ over one day or more) (Hicks et al. 1984).

5. Assembly phase

The prototype mechanical parts have been realized in-house in stainless steel. We selected stainless steel for its stiffness properties, low cost and availability. The two concentric rings of the movable plate have been realized with a maximum surface error $< 40\mu m$ over the whole surface. The mechanical parts of the prototype has been assembled in the laboratory as well as the micrometers, the piezo-actuators, the capacitive sensors and the optical plates (Fig. 3). At present, two preliminary sets of optical plates have been manufactured by LightMachinery, with $\lambda/30$ and $\lambda/60$ surface errors, respectively.

6. Conclusions and future developments

We have presented the design of a laboratory prototype Capacitance Stabilized Fabry-Pérot interferometer. We presented an effective FP numerical model. Simulation results allowed to design a FP prototype optimized for the scan of the H_α line, but also suitable for the whole visible range. We have presented the mechanical, electronic and optical characteristics of the prototype components and described the solution adopted in the prototype design and its assembly. In the near future, we plan to perform the full optical and spectral qualification tests.

Furthermore, we are working on a space implementation of the FP in order to start space qualification tests. The FP design has been update to match the more demanding operating environment requirements, such as the launch stresses and the larger thermal variations.

References

Berrilli, F., et al. 2009, MmSAI, 80, 251

Berrilli, F., et al. 2010, Advances in Space Research, 45, 1191

Berrilli, F., et al. 2011, Proc. SPIE, 8148,

Born, M., & Wolf, E. 1999, Principles of Optics, Cambridge University Press, pp. 986

Giovannelli, L., Berrilli, F., et al. 2012, Proc. SPIE, 8446,

Greco, V., Cavallini, F., & Berrilli, F. 2010, Proc. SPIE, 7731,

Hicks, T. R., Reay, N. K., & Atherton, P. D. 1984, Journal of Physics E Scientific Instruments, 17, 49

Kameda, S., et al. 2010, 38th COSPAR Scientific Assembly, 38, 746